

**Stochastic Ion Heating by a Perpendicularly  
Propagating Electrostatic Wave\***

C. F. F. Karney and A. Bers

Plasma Research Report

PRR 76/35-1

*Revised: Jan. 21, 1977*

**\*Work supported by U.S. Energy Research and Development Administration (Contract E(11-1)-3070)**

***Submitted to Physical Review Letters.***

## Stochastic Ion Heating by a Perpendicularly Propagating Electrostatic Wave\*

C. F. F. Karney and A. Bers

*Research Laboratory of Electronics and Plasma Fusion Center,  
Massachusetts Institute of Technology, Cambridge, Massachusetts 02139*

### *Abstract.*

The motion of an ion in the presence of a constant magnetic field and a perpendicularly propagating electrostatic wave with frequency several times the ion cyclotron frequency is shown to become stochastic for fields satisfying  $E/B_0 > \frac{1}{4} (\Omega/\omega)^{1/3} (\omega/k)$ . This stochasticity condition is independent of how close  $\omega$  is to a cyclotron harmonic. Applications of current interest in supplementary heating of plasmas with RF power near the lower hybrid frequency are suggested.

*Stochastic Ion Heating by a Perpendicularly Propagating Electrostatic Wave.*

It is well known that a small (infinitesimal) amplitude electrostatic wave traveling across a constant magnetic field suffers linear damping on the ions only if its frequency  $\omega$  is an exact multiple of the ion cyclotron frequency,  $\Omega$ . At finite amplitudes of the wave, nonlinear effects become important and we can expect that this resonance is broadened. We show that a single wave leads to stochastic ion motion at an amplitude which is independent of how close  $\omega$  is to a cyclotron harmonic,  $n\Omega$ . This provides a mechanism whereby the ions in a plasma can be heated by such coherent waves.

There are two, physically distinct, nonlinear mechanisms operative in this interaction. The first consists of a transient trapping of the ions in the potential of the wave; this leads to a rapid heating of the ions near the lower boundary of the stochastic region.<sup>1</sup> The second is due to nonlinear resonances that arise from the perturbed cyclotron motion of the ions in the wave field, and which produce stochastic ion motion in a region of ion velocity space extending from the trapping region to an upper bound determined by the field amplitude; this leads to a slower heating of the ions up to the upper boundary of the stochastic region.

In current schemes for the supplementary heating of tokamak plasmas with microwave power, wavepacket fields that propagate nearly across the magnetic field (e.g. lower hybrid resonance cones and some of their parametrically excited decay waves) are generated. The stochastic ion heating mechanism we present can play an important role in such heating schemes.

Stochastic ion motion can also be caused by an obliquely propagating wave, that traps ions in the potential wells parallel to the magnetic field.<sup>2</sup> This mechanism is inapplicable for the wave of interest here, which we take to propagate exactly across the magnetic field.

We consider an ion in a constant magnetic field  $B_0 \hat{z}$  and a perpendicularly propagating electrostatic wave  $\hat{y}E \cos(ky - \omega t - \phi)$ . The equations of motion are

$$\ddot{y} + y = \alpha \cos(y - \nu t - \phi), \quad \dot{x} = y, \quad (1)$$

where lengths are normalized to  $k^{-1}$  and times to  $\Omega^{-1}$ ,  $\alpha = qkE/(m\Omega^2)$  and  $\nu = \omega/\Omega$ . (Without loss of generality, the constant of the motion  $\dot{x} - y$  is set equal to zero.) The Hamiltonian for this system is

$$H = I_1 + \nu I_2 - \alpha \sin[(2I_1)^{1/2} \sin w_1 - w_2], \quad (2)$$

where  $(I_1, w_1)$  and  $(I_2, w_2)$  are conjugate action-angle variables and  $y = (2I_1)^{1/2} \sin w_1$ . The variables  $(I_2, w_2)$  have been introduced to make  $H$  time independent. In (2)  $w_2$  is the wave phase and so  $H$  describes two harmonic oscillators, the ion in a magnetic field described by  $(I_1, w_1)$  and the wave described by  $(I_2, w_2)$ , coupled by the last term in (2).

In order to find the condition for the onset of stochasticity we use the surface of section method.<sup>3</sup> We choose the cross section defined by  $w_1 = \pi$  and numerically compute  $r \equiv (2I_1)^{1/2}$ , the normalized velocity, against  $w_2$  for each crossing of the  $w_1 = \pi$  plane. Fig. 1 shows the results of such computations for  $\nu = 30.23$ ,  $\alpha = 2.2$  and 4, and in a region of velocity space with  $r > \nu$ . With  $\alpha = 0$  the trajectories would all lie on horizontal straight lines, since  $I_1$  is a conserved quantity. At  $\alpha = 2.2$  the trajectories have become quite complex, many lying on chains of "islands." The order of the islands is given by the number of cyclotron orbits it takes for the ion to return to the island it started on. Clearly visible are chains of fourth and fifth order islands. Outside the islands the motion appears stochastic, but the stochastic regions are separated from one another by coherent regions, preventing the movement of particles from one stochastic region to another and limiting the amount of energy the particles can gain. Finally at  $\alpha = 4$ , the stochastic regions have merged allowing particles to be heated through the region of velocity space shown in the figure. In this case the destruction of the coherent region is caused by the appearance of a chain of third order islands. We define the field at which the stochastic regions merge as the "stochasticity threshold."

From the study of these figures and others at different frequencies, we form the following picture of how the motion becomes stochastic: The presence of the wave causes a nonlinear change in the cyclotron frequency,  $\langle \dot{w}_1 \rangle$ . This in turn causes the ratio of the wave frequency to the cyclotron frequency to become a "simple" rational number in certain regions of velocity space, leading to fixed points. [In Fig. 1(a), for instance, the cyclotron frequency has become  $\nu/(30\frac{1}{4})$  and  $\nu/(30\frac{1}{5})$  at the fourth and fifth order islands, respectively.] Around half of these fixed points, islands form; the other half are hyperbolic fixed points at the separatrices between the islands. As is well known,<sup>3,4</sup> the addition of any small perturbation to the system causes the motion in the vicinity of the separatrix to become stochastic. As the field is increased the size of the stochastic regions surrounding the islands increases, and islands of different orders appear which eventually destroy enough of the coherent motion to allow particles to be heated.

To find the scaling of the stochasticity threshold, we must find the conditions under which islands can form. The location of  $p$ 'th order islands may be derived analytically by finding  $p$ 'th order fixed points. These in turn are found by setting

$$\langle \dot{w}_1 \rangle / \dot{w}_2 = \langle \dot{w}_1 \rangle / \nu = p/s, \quad (3)$$

where  $s$  and  $p$  are integers and the (time) average is performed over  $p$  cyclotron orbits (or, equivalently,  $s$  wave periods). For first order islands ( $p = 1, s = n$ ),  $\langle \dot{w}_1 \rangle$  is readily found by Fourier-transforming the last term in (2). Then to order  $\alpha$ ,  $nw_1 - w_2$  is constant, and so only one term in the Fourier sum contributes to give

$$\langle \dot{w}_1 \rangle = 1 - \alpha (\partial/\partial I_1) J_n [(2I_1)^{1/2}] \sin(nw_1 - w_2). \quad (4)$$

To find the threshold for first order islands we substitute (4) in (3) and take  $\sin(nw_1 - w_2) = \pm 1$ . If we also asymptotically expand the Bessel function we obtain

$$\alpha = (\pi r^3/2)^{1/2} |\delta|/n, \quad (5)$$

where  $\nu = n + \delta$ . For  $p \neq 1$ , we transform<sup>5</sup>  $H$  to a set of action-angle variables for which the angles are cyclic to order  $\alpha$ . To order  $\alpha^2$ , there are contributions to  $H$  varying as  $\sin(mw_1 - kw_2)$ , where  $k = 0$  or  $2$ . If  $p \neq 2$  then on averaging only the angle independent term ( $m = k = 0$ ) contributes giving

$$\langle \dot{w}_1 \rangle = 1 - \frac{\alpha^2}{4} \sum_{m=-\infty}^{\infty} \frac{\partial^2 J_m^2 [(2I_1)^{1/2}]}{\partial I_1^2} \frac{m}{m - \nu}. \quad (6)$$

For  $p = 2$ , there is an additional contribution when  $m = s$  and  $k = 2$ ; however, in the limit  $r \gg \nu$ , this term is negligible, so we use (6) in this case also. The threshold for higher order islands is again obtained by substituting in (3). Asymptotically expanding the Bessel functions, and assuming  $\nu \gg 1$  this gives

$$\alpha = |\sin(\pi \delta) \epsilon r^3|^{1/2} / n, \quad (7)$$

where  $\nu = s/p + \epsilon$ .

In Fig. 2 we plot the predicted values of the thresholds for island formation as given by (5) and (7) for  $29\frac{1}{2} < \nu < 30\frac{1}{2}$ , and  $r \approx 47.5$  (in this plot we have allowed for the fact that  $r \gg \nu$  is not satisfied), together with the numerically observed thresholds for various  $\nu$ . We note that for large  $\alpha$ , island chains of many different orders are predicted. Also given in Fig. 2 are some numerically observed stochasticity thresholds. We observe that this threshold is insensitive to  $\delta$ , varying by about 20% for  $\delta$  between  $-\frac{1}{2}$  and  $\frac{1}{2}$ . Since the islands cause the motion to become stochastic, an accurate expression for the stochasticity threshold is obtained merely by replacing  $\delta$  and  $\epsilon$  in (5) or (7) by constants, giving, for  $r \gg \nu \gg 1$ ,

$$\alpha = (\pi r^3 / 2)^{1/2} / (4n). \quad (8)$$

For  $r \approx \nu$ , we must go back to (4) and (6) and expand in the limit  $\nu \gg 1$  to obtain<sup>6</sup>

$$\alpha = \nu^{2/3}/4, \quad (9)$$

or, in unnormalized terms,

$$E/B_0 = \frac{1}{4} (\Omega/\omega)^{1/3} (\omega/k). \quad (10)$$

Our results can be used to determine what region of velocity space is stochastic for a given  $\alpha$ . For  $\alpha$  much larger than the threshold given by (9), the upper limit may be found by inverting (8) to give

$$r = (4\alpha n)^{2/3} (2/\pi)^{1/3}. \quad (11)$$

The lower limit is determined by trapping<sup>1</sup> and so is given by

$$r = \nu - \sqrt{\alpha}. \quad (12)$$

Fig. 3(a) shows these limits for  $\nu = 30.23$ , together with the numerically observed values. How an ion gains energy within the stochastic region may be illustrated by integrating the equations for a number of ions with velocities just above the lower limit of the stochastic region and with evenly distributed phases. In Fig. 3(b) we plot the rms speed of 50 particles as a function of cyclotron orbit number (which is nearly proportional to time) for  $\alpha = 20$  and  $\nu = 30.23$ . We note that the fairly rapid initial energy gain is followed by a slower heating. We can attribute the initial energy gain to the effects of trapping. Indeed, the rms velocity after the first few cyclotron orbits is close to  $\nu + 2\sqrt{\alpha}$ . The slow heating continues for longer than 1000 cyclotron orbits, at which time the rms velocity is about 90, and the velocity distribution function has spread over most of the stochastic region, Fig. 3(c).

As an example, consider a wave near the lower hybrid frequency in a plasma with  $n_0 = 10^{14}$  cm<sup>-3</sup>,  $B_0 = 50$  kG and  $T_i = 1$  keV. Taking  $\omega/\Omega_i = \nu = 24$ , and  $k_{\perp} v_{Ti}/\Omega_i = 6$ , then from (10) the threshold field for stochasticity is about 5.5 kV/cm [at this field  $\epsilon_0 E^2/(4n_0 T_i)$  is about  $4 \times 10^{-5}$ ].

The motion becomes stochastic for particles traveling at the wave phase velocity which is  $4v_{Ti}$  so that an appreciable number of tail particles is heated. In tokamaks the lower hybrid wave is of finite extent, determined by the excitation structure. In this example, if the extent along  $B_0$  is 10 cm, then the ions spend about 20 cyclotron periods in this field and can increase their energy by an amount corresponding to the trapping width of the fields. At much higher amplitudes of the lower hybrid fields, the conditions for parametric decay may also be satisfied. For the decay waves which are of lower frequency and shorter wavelength, the conditions for stochastic ion-heating (10) and (12) may be more readily satisfied even for ions with velocities nearer to  $v_{Ti}$  so that bulk ion heating can result.

References and Footnotes.

\*Work supported by U.S. Energy Research and Development Administration (Contract E(11-1)-3070)

<sup>1</sup>C. F. F. Karney, A. Bers, and D. C. Watson, *Bull. Am. Phys. Soc.*, 20, 1313 (1975), and C. F. F. Karney and A. Bers, *Plasma Research Reports* 76/7 (Jan. 1976) and 76/24 (July 1976), Research Laboratory of Electronics, Massachusetts Institute of Technology.

<sup>2</sup>G. R. Smith and A. N. Kaufman, *Phys. Rev. Lett.* 34, 1613 (1975).

<sup>3</sup>G. M. Zaslavskii and B. V. Chirikov, *Usp. Fiz. Nauk* 105, 3 (1971) [*Sov. Phys. - Usp.* 14, 549 (1972)].

<sup>4</sup>J. Ford, *The Statistical Mechanics of Classical Analytic Dynamics*, in *Fundamental Problems in Statistical Mechanics, Vol 3*, Editor E. D. G. Cohen (North-Holland Publishing Co., Amsterdam, Neth. 1975).

<sup>5</sup>G. H. Walker and J. Ford, *Phys Rev.* 188, 416 (1969)

<sup>6</sup>This result may also be obtained (to within a factor of order unity) by demanding that trapping be effective, in the sense that an ion in its orbit spend at least a bounce period ( $2\pi\alpha^{-1/2}$ ) within the trapping region given by  $|\dot{y} - v| < \sqrt{\alpha}$ .

## Figure Captions.

FIG. 1. The  $w_1 = \pi$  cross-sections of phase space for  $\nu = 30.23$  and (a)  $\alpha = 2.2$ , (b)  $\alpha = 4$ . The trajectories of 24 particles are followed for 300 orbits in each case. Crosses (x) indicate initial conditions, dots (·) subsequent crossings. In (a) the numbers indicate the position of fourth and fifth order islands and the order in which they are visited. The initial conditions were picked to illustrate the dominant features of the motion.

FIG. 2. The threshold  $\alpha$  for the formation of islands of various orders (the numbers by the curves) for  $r \approx 47.5$  as a function of  $\nu$ . The lines give the analytically predicted values and the crosses (x) the numerically observed values. The plusses (+) give the numerically observed stochasticity thresholds.

FIG. 3. (a) The limits of the stochastic region as given by (9), (11), and (12). The crosses (x) give the numerically observed values. The terms "Disconnected Stochastic" and "Connected Stochastic" are used to distinguish motion of the type shown in Fig. 1(a) and Fig. 1(b), respectively. (b) Heating of a group of 50 particles with  $\alpha = 20$ , initial velocity  $r = 23$ , and evenly distributed phases. (c) Velocity ( $r$ ) distribution function for the particles in (b) averaged over orbits 800 - 1100. Normalization is such that  $\int 2\pi r f dr = 1$ .

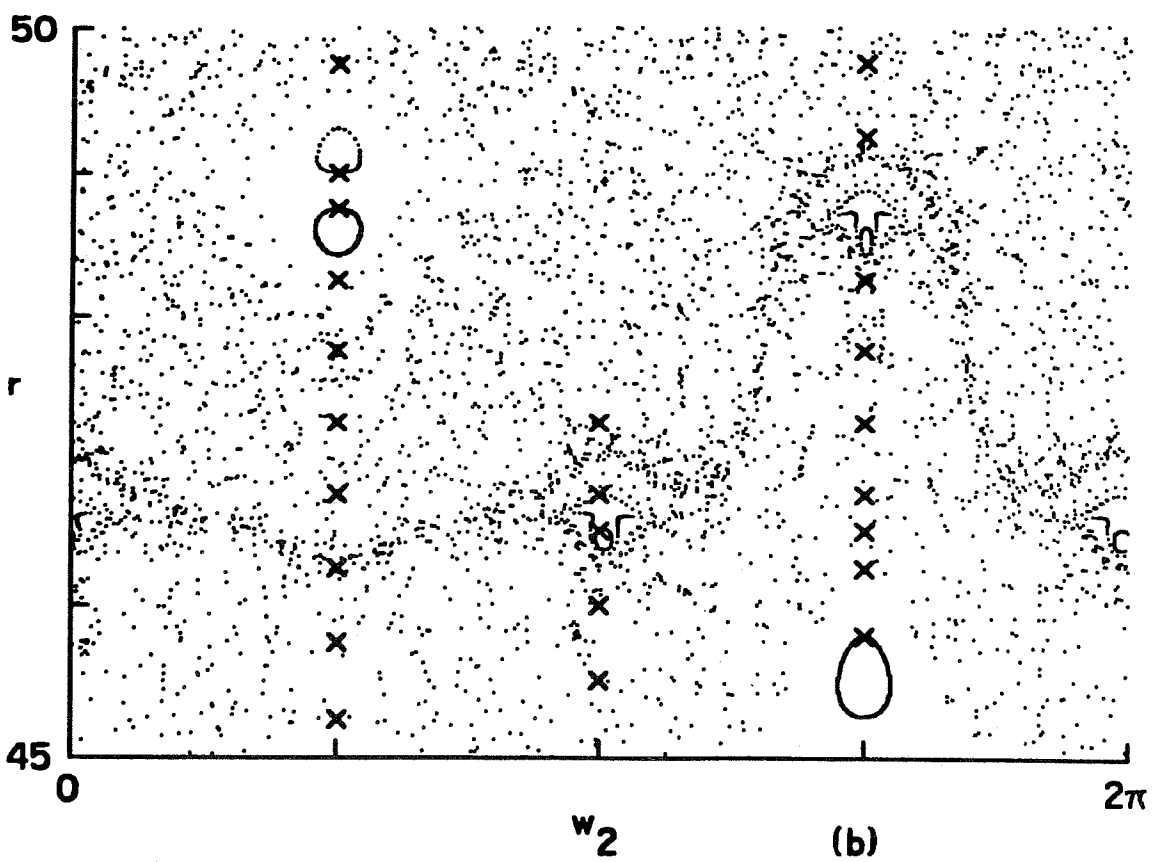
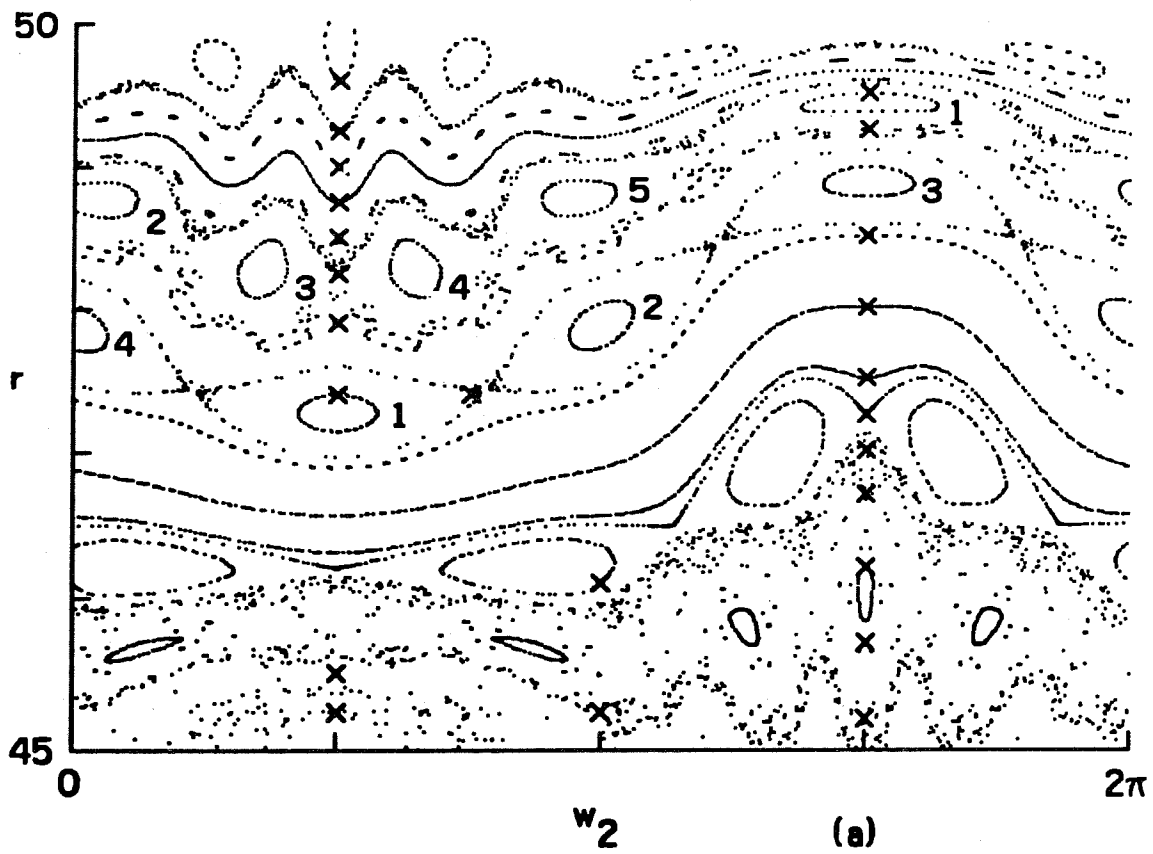


FIGURE 1

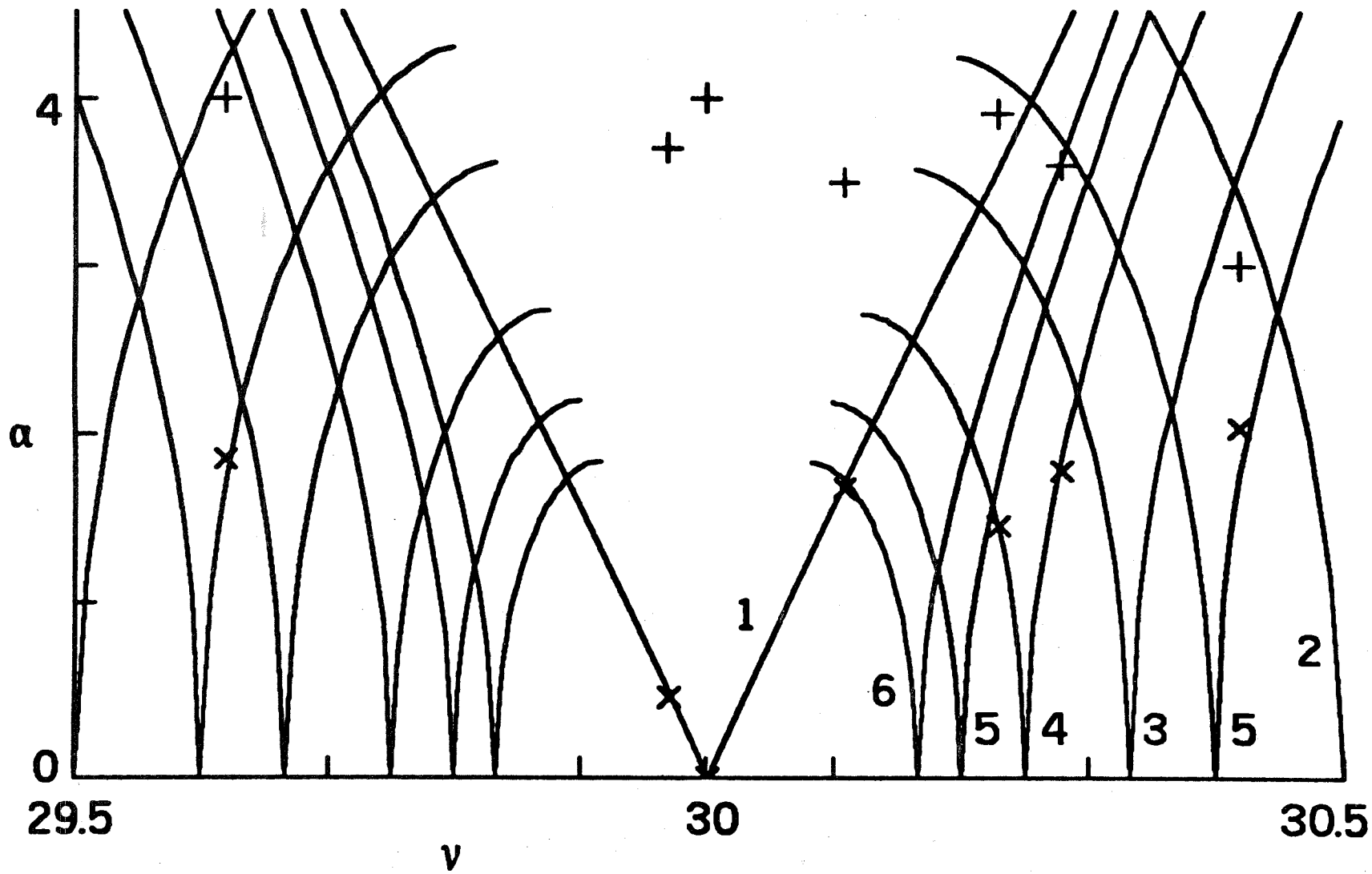


Figure 2

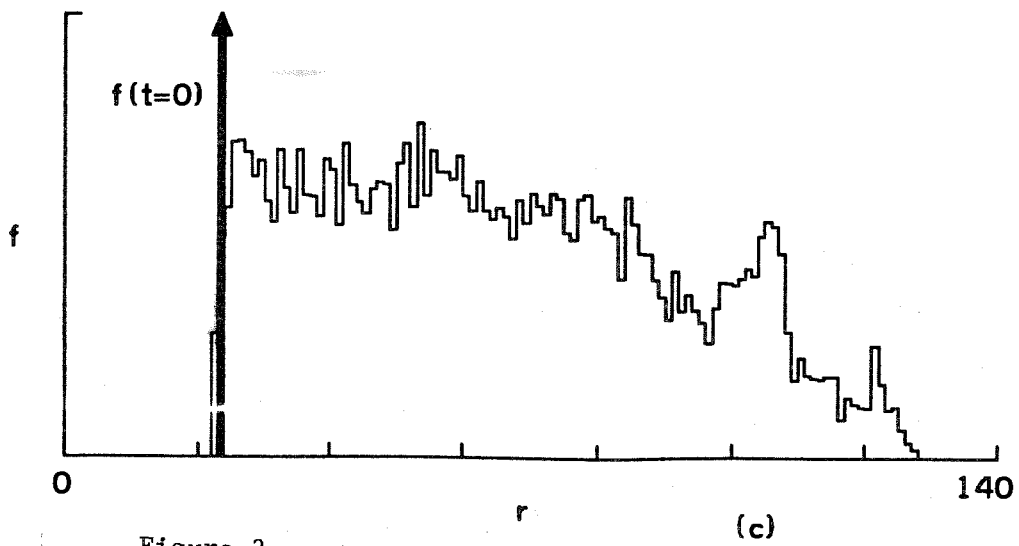
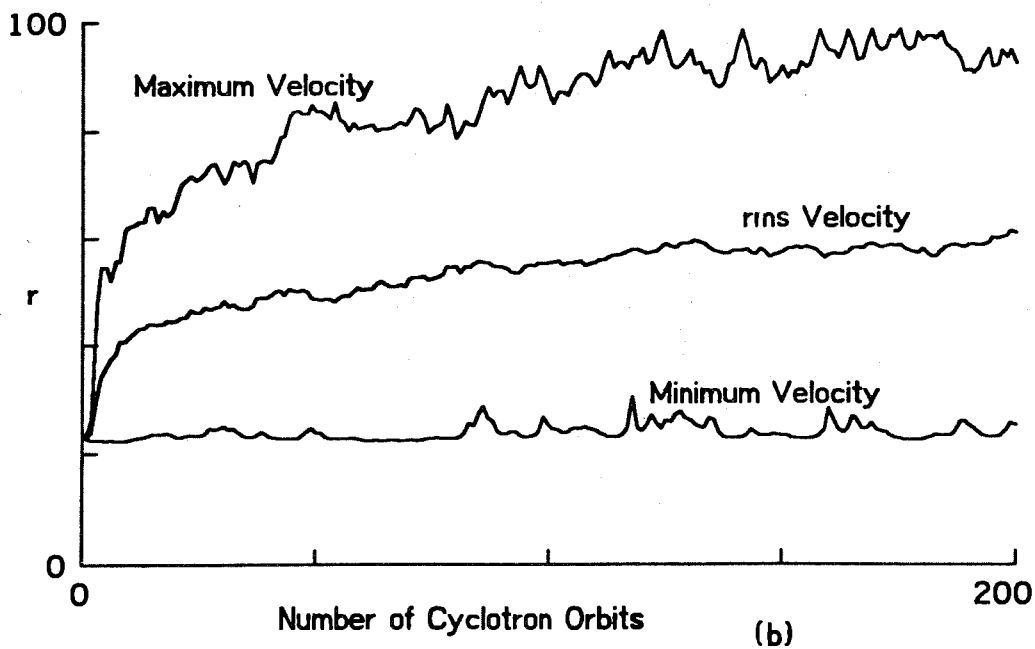
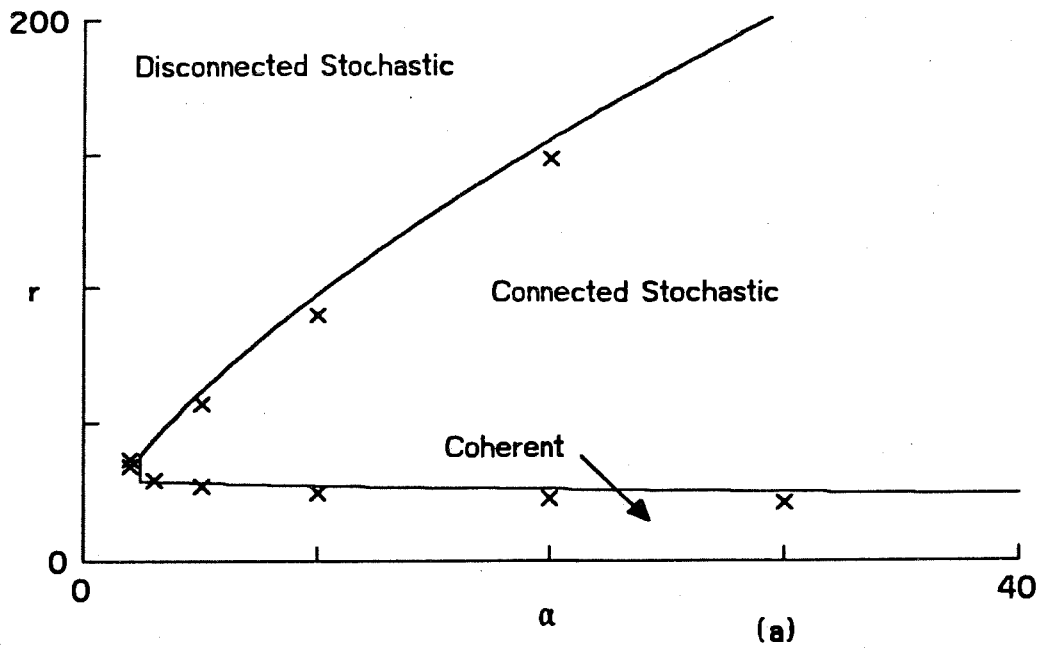


Figure 3